PHYSICS OF FLUIDS
(Formerly Physics of Fluids A)

Vol. 6, No. 2, Pt. 2 February 1994

Nonlinear interactions between oblique instability waves on nearly parallel shear flows

M. E. Goldstein
National Aeronautics and Space Administration, Lewis Research Center, Cleveland, Ohio 44135

pp. 724-735

AMERICAN INSTITUTE OF PHYSICS

Nonlinear interactions between oblique instability waves on nearly parallel shear flows

M. E. Goldstein
National Aeronautics and Space Administration, Lewis Research Center, Cleveland, Ohio 44135

(Received 9 March 1993; accepted 25 May 1993)

Asymptotic methods are used to describe the nonlinear self-interaction between a pair of oblique instability modes that eventually develops when initially linear, spatially growing instability waves evolve downstream in nominally two-dimensional, unbounded or semibounded, laminar shear flows. The first nonlinear reaction takes place locally within a so-called "critical layer" with the flow outside this layer consisting of a locally parallel mean flow plus a pair of oblique instability waves together with an associated plane wave. The instability wave amplitudes, which are completely determined by nonlinear effects within the critical layer, satisfy a pair of integral differential equations with quadratic to quartic-type nonlinearities. The most important feature of these equations is the oblique mode, self-interaction term that usually leads to a singularity at a finite downstream position. It is shown that this type of interaction is quite ubiquitous and is the dominant nonlinear interaction in many apparently unrelated shear flows—even when the oblique modes do not exhibit the most rapid growth in the initial linear stage.

I. INTRODUCTION

This paper is mainly a review and synthesis of some recent developments in nonlinear stability theory [but some new results, such as Eqs. (39)–(43), are also derived]. It is concerned with the first nonlinear interactions that come into play when a pair of spatially growing and initially linear oblique instability waves evolve downstream in nominally two-dimensional, unbounded or semibounded, laminar shear flows. There are, of course, numerous studies of oblique-mode interactions in the literature (e.g., Goldstein and Choi;[1] Chang and Malik,[2] Thumm, Wolz, and Fasel;[3] Goldstein and Choi,[1] Chang and Malik,[2] and Wu, Lee, and Cowley[4] consider the interaction of two oblique modes, while Craik,[5] Goldstein and Lee,[6] Herbert,[7] Spalart and Yang,[8] and Wu[9] consider the interaction of two oblique modes with a plane wave), but this review is only concerned with the rigorously based analytical treatments, i.e., the ones that use a systematic asymptotic approach to study these interactions. Comparison with experiment will be discussed in a forthcoming paper and is not considered herein.

The instability waves are (for definiteness) assumed to arise from some sort of small-amplitude, time-harmonic excitation device, as indicated schematically in Fig. 1. This means that the initial motion just downstream of this device will also have harmonic time dependence and be well described by linear instability wave theory. The Reynolds number R is assumed to be large enough so that the flow is nearly parallel.

While the peak linear growth rate is usually of the same order as the inverse shear-layer thickness Δ^{-1} in highly unstable flows, such as free shear layers, jets, and (usually separated) wall boundary layers with $O(1)$ adverse-pressure gradients, it is usually small compared to Δ^{-1} in more stable flows, such as flat-plate boundary layers or unseparated boundary layers with weak adverse-pressure gradients. However, mean flow divergence effects will usually cause the growth rate to be small (relative to Δ^{-1}) by the time nonlinear effects set in, even in the more unstable flows. This is because, in the latter type of flows, the excitation is usually located in the vicinity of the peak local growth rate, of the relevant normalized instability growth-rate curve—such as the one shown schematically in Fig. 2. The growth rate should therefore decrease as the instability waves propagate downstream into a region where (in most cases) the shear-layer thickness Δ will have increased.

This suggests that the method of matched asymptotic expansions can be used to describe these flows: with an "inner" nonlinear region, in which the instability-wave growth rate is small, and a much larger "outer" region in which the unsteady flow is governed by linear dynamics, but in which mean-flow divergence effects are important (see Fig. 3). A uniformly valid composite solution that applies everywhere in the linear and nonlinear regions can then be obtained in one of the usual ways—say, by multiplying the linear and nonlinear solutions together and then dividing through by their common part in the overlap domain (that always exists between the inner and outer regions).

II. THE OUTER LINEAR FLOW

We begin by considering the initial linear stage just downstream of the excitation device. In some flows, such as supersonic free shear layers, or flat-plate boundary layers in the relatively low, supersonic Mach number regime, where the so-called, first-mode instability is dominant, the most rapidly growing mode is, in fact, an oblique wave, so that the oblique-mode self-interaction that is of interest herein is likely to be the first nonlinear interaction to occur.

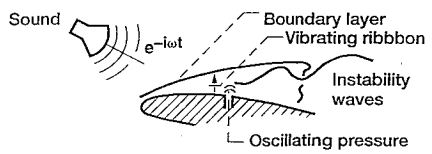

2-D Unseparated boundary layer on thin body.

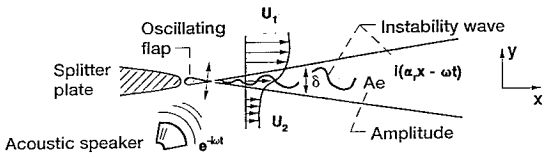

Mixing layer between two parallel streams

FIG. 1. Typical shear flow configurations.

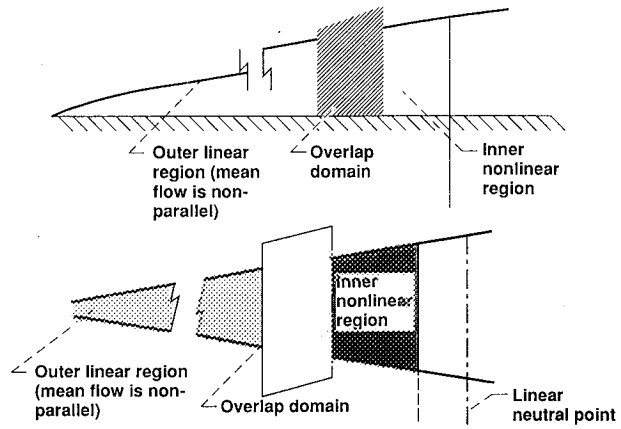

FIG. 3. Asymptotic structure of flow.

In which case, it is reasonable to begin the unsteady motion with a pair of oblique (equiamplitude) instability-wave modes with the same streamwise wave number $\alpha_r/2$ and scaled frequency $\omega^*\Delta/2U_\infty = \alpha_r c_r/2$ and equal and opposite spanwise wave numbers ($\pm\beta$). (Here U_∞ is the characteristic velocity of the flow, and the subscript r is used to denote the real part of the wave number α and phase speed c, as well as other quantities to which it is appended.) These two waves combine to form a standing wave in the spanwise direction that propagates only in the direction of flow—which is the situation that most frequently occurs in wave excitation experiments that typically involve longish excitation devices placed perpendicular to the flow.

However, in most flows, it is the plane wave that exhibits the most rapid growth in the initial linear stage, even though the oblique modes ultimately exhibit the most rapid growth upon entering some intermediate (parametric resonance) stage. This intermediate stage can be treated simultaneously with the self-interaction stage (which is of interest here) if we begin the unsteady motion with a resonant triad of instability waves in the initial linear region—a plane fundamental frequency wave, with scaled frequency $\omega^*\Delta/U_\infty$, and a pair of oblique equiamplitude subharmonic waves, (again) with the same streamwise wave number and frequency, $\frac{1}{2}\alpha_r$ and $\frac{1}{2}\alpha_r c_r$, respectively, and equal but opposite spanwise wave numbers $\pm\beta$.

For present purposes, the term "resonance" simply means that the three waves all have the same phase speed c_r. For the small growth rates and large Reynolds numbers that are of interest here, this occurs when

$$\beta = (\sqrt{3}/2)\alpha_r, \tag{1}$$

which means that the oblique instability waves make a 60° angle with the direction of flow. We can, of course, allow that angle to be arbitrary in flows where the oblique modes can grow more rapidly than the plane wave and resonant reaction with the latter is not required to enhance the growth rate of the former. Our choice of the initial linear modes may seem somewhat artificial, but the linear and parametric resonance stages act as narrow-band filters that are able to select out these disturbances from relatively generic background disturbance fields. Moreover, we eventually show (at the end of Sec. III) that the resonance condition (1) does not have to be satisfied exactly and that the analysis actually applies to a fairly broad range of wave numbers about the resonant condition.

Since our scaling requires that the instability-wave growth rates be small in the nonlinear region of the flow, and since the Reynolds number R is assumed to be large, the first modal interaction is confined to a localized region centered around the "critical level" where the mean-flow velocity, say U_c, is equal to the common phase velocity c_r of the two or three modes that interact there (see Fig. 4). The flow outside this so-called "critical layer" is still governed by linear dynamics, which means that it is given by a locally parallel two-dimensional mean flow, say $U(y)$, plus a pair of oblique instability-wave modes along with a plane (i.e., two-dimensional) instability wave. There is also

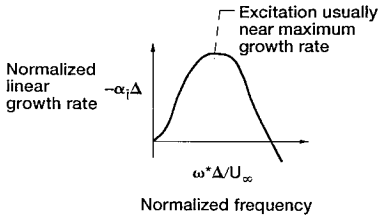

FIG. 2. Typical linear growth rate curve.

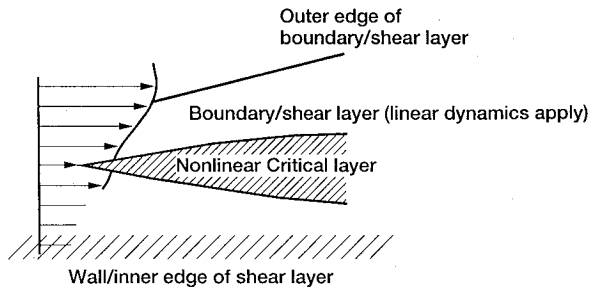

FIG. 4. Structure of the nonlinear region.

a spanwise variable mean-flow distortion—to be discussed more fully below—that is generated by nonlinear effects within the critical layer.

The (external) transverse velocity fluctuation v is then given by

$$v=-\epsilon\sigma\bar{\alpha}\,\mathrm{Re}\left[\sec\theta A(x_0)\Phi(y)e^{iX/2}\cos Z + \left(\frac{\epsilon}{\sigma}\right)^{1/3}A_0(x_0)\Phi_0(y)e^{iX}\right], \tag{2}$$

where

$$X\equiv\sigma\bar{\alpha}(x-\sigma\bar{c}t), \tag{3}$$

$$Z\equiv\sigma\bar{\beta}z, \tag{4}$$

$$\alpha=\sigma\left[\bar{\alpha}+O\left(\frac{\epsilon}{(1+\lambda)\sigma}\right)^{1/3}\right], \tag{5}$$

$$c=\sigma\left[\bar{c}+O\left(\frac{\epsilon}{(1+\lambda)\sigma}\right)^{1/3}\right], \tag{6}$$

$$c_0=\sigma\left[\bar{c}+O\left(\frac{\epsilon}{(1+\lambda)\sigma}\right)^{1/3}\right], \tag{7}$$

$$x_0=\sigma\left(\frac{\epsilon}{\sigma}\right)^{1/3}x, \tag{8}$$

$$\theta\equiv\tan^{-1}\left(\frac{2\bar{\beta}}{\bar{\alpha}}\right). \tag{9}$$

and Re denotes the real part. The streamwise, transverse, and spanwise coordinates, normalized by the shear-layer thickness Δ, are x, y, and z, respectively; t denotes the normalized time; and θ denotes the propagation angle of the oblique mode. The scaled spanwise wave number, streamwise wave number, and phase speed $\bar{\beta}$, $\bar{\alpha}$, and $\bar{c}$, respectively, are purely real. The first term in this equation [i.e., Eq. (2)] represents the oblique modes, while the second represents the plane wave. Here Φ and Φ_0, are the linear normal mode shapes which can, in general, be found by solving the appropriate Rayleigh equation (but, see below). Also, A and A_0, which depend only on the streamwise coordinate (and then only through the scaled streamwise variable x_0, which varies on the length scale of the nonlinear region which, not very surprisingly, turns out to be the reciprocal instability-wave growth rate) determine the overall growth of the instability waves and are, therefore, the most important quantities in these equations. They are completely determined by the nonlinear dynamics within the critical layer and are, in practice, found by equating the velocity jump across the critical layer, as calculated from the external linear solution (i.e., the solution to Rayleigh's equation), to the velocity jump calculated from the internal nonlinear solution within the critical layer. The amplitude scale factors for the oblique and plane waves are ϵ and $\epsilon(\epsilon/\sigma)^{1/3}$, respectively, where ϵ is always much less than σ.

Notice that the growth rate and oblique mode amplitude scalings $\sigma(\epsilon/\sigma)^{1/3}$ and ϵ, respectively, are related. This relation ensures that growth rate and nonlinear (or mode interaction) effects will both impact the external linear solution at the same asymptotic order. It is dictated by the requirement that the nonlinear stage correspond to the first stage of evolution beyond the initial linear region, i.e., that the nonlinear solutions match onto the upstream linear solutions in the matched asymptotic sense. The Benney–Bergeron[11] parameter

$$\lambda\equiv 1/\epsilon\sigma^3R, \tag{10}$$

where R is the Reynolds number based on the shear layer thickness Δ, is (in the present context) a measure of the relative importance of viscous to growth-rate effects within the critical layer, i.e., these effects will be of the same order when $\lambda=O(1)$.

The wavelength scale factor σ can be set to unity when the initial linear instability wave has an order-one wavelength. In which case the linear, instability-wave growth rate will be[1] $O(\epsilon^{1/3})$ as the nonlinear region is approached (which fixes the location of this region). This will usually be the case for highly unstable flows such as free shear layers and (usually separated) boundary layers with order-one, adverse-pressure gradients.

For somewhat more stable flows, such as boundary layers with sufficiently small pressure gradients [$=O(\sigma^2)$], σ will be small compared to unity, and the linear growth rate will scale like σ^4 over most of the unstable region.[6] The nonlinear critical-layer effects will therefore come into play over most of the unstable region (and not just near the neutral curve), if we take

$$\sigma\left(\frac{\epsilon}{\sigma}\right)^{1/3}=\sigma^4 \quad \text{when } \lambda=O(1),$$
$$\sigma\left(\frac{\epsilon}{\lambda\sigma}\right)^{1/3}=\sigma^4 \quad \text{when } \lambda\to\infty. \tag{11}$$

And for even more stable flows, such as accelerating boundary layers[9,12] with $O(1)$ pressure gradients, the growth rate will be $O(\sigma^2)$ over the main part of the unstable region. In which case, the nonlinear critical-layer effects will come into play in the major portion of this region if we take

$$(\epsilon/\lambda\sigma)^{1/3}=\sigma \quad \text{as } \lambda\to\infty. \tag{12}$$

Finally, we note that the phase speeds of the oblique and plane-wave modes, c and c_0 respectively, will only be equal (i.e., resonance will only occur) if $\bar{\alpha}$ and $\bar{\beta}$ satisfy (1), or equivalently if α and β satisfy (1) to within order $\sigma[\epsilon/(1+\lambda)\sigma]^{1/3}$.

III. CRITICAL-LAYER DYNAMICS AND THE AMPLITUDE EQUATIONS

The lowest-order critical-layer equations turn out to be linear and correspond to a balance between growth rate (i.e., nonequilibrium), mean-flow convection, and viscous–diffusion effects. Benney and Maslowe[13] were the first to

show that nonlinear and nonequilibrium effects could simultaneously enter the critical-layer equations. Here the nonlinearity is weak in the sense that it does not affect the lowest-order equations, but enters only through inhomogeneous terms in a higher-order problem. This ultimately means that the all-important amplitude functions A and A_0 can be determined from a single pair of amplitude equations. The relevant equations—corresponding to the generalized scaling (3)–(8)—can easily be inferred from the specific results of Refs. 1, 6, 4, and 33. They are

$$\frac{d\tilde{A}(\tilde{x})}{d\tilde{x}}=\tilde{\kappa}\tilde{A}(\tilde{x})+i\int_{-\infty}^{\tilde{x}}K_1\tilde{A}_0(x_1)\tilde{A}^*(2x_1-\tilde{x})dx_1+i\tilde{\gamma}\int_{-\infty}^{\tilde{x}}\int_{-\infty}^{x_1}K_2\tilde{A}(x_1)\tilde{A}(x_2)\tilde{A}^*(x_1+x_2-\tilde{x})dx_2\,dx_1, \tag{13}$$

$$\frac{d\tilde{A}_0(\tilde{x})}{d\tilde{x}}=\tilde{\kappa}_0\tilde{A}_0(\tilde{x})+i\tilde{\rho}\tilde{\gamma}\int_{-\infty}^{\tilde{x}}\int_{-\infty}^{x_1}[K_3\tilde{A}_0(x_1)\tilde{A}(x_2)\tilde{A}^*(2x_1+x_2-2\tilde{x})+K_4\tilde{A}(x_1)\tilde{A}_0(x_2)\tilde{A}^*(x_1+2x_2-2\tilde{x})]dx_2\,dx_1$$
$$+i\tilde{\rho}\tilde{\gamma}^2\int_{-\infty}^{\tilde{x}}\int_{-\infty}^{x_1}\int_{-\infty}^{x_2}K_5\tilde{A}(x_1)\tilde{A}(x_2)\tilde{A}(x_3)\tilde{A}^*(x_1+x_2+x_3-2\tilde{x})dx_3\,dx_2\,dx_1, \tag{14}$$

where the asterisks denote complex conjugates, $\tilde{x}$, $\tilde{A}$, and $\tilde{A}_0$ are suitably renormalized, and shifted variables corresponding to x_0, A, and A_0, respectively, and $\tilde{\rho}$ and $\tilde{\gamma}(|\tilde{\gamma}|=1)$ are complex parameters which are dependent on the basic mean flow. The scaled linear growth rates of the oblique and plane modes are $\tilde{\kappa}$ and the real part of $\tilde{\kappa}_0$, respectively. The imaginary part of $\tilde{\kappa}_0$, $\tilde{\kappa}_{0i}$, represents the initial phase shift between the oblique and plane-wave modes.

Notice that these are integrodifferential equations of the type first obtained by Hickernell[10] rather than the usual ordinary differential equations that arise in classical Stuart–Watson–Landau[14–16] theory. The integrals arise from upstream history effects that produce a gradual phase shifting between modes when the nonlinearity takes place within a nonequilibrium (or growth dominated) critical layer. This occurs because the evolution or growth-rate effects have a dominant (i.e., first-order) effect on the flow within the critical layer, but only weakly affect the flow outside the critical layer. The nonlinear terms are therefore influenced by the growth-rate effects when they are generated within the critical layer, but not when they are generated outside the critical layer, as in the classical theory. The nonlinear kernel functions K_1 through K_5 will be described subsequently. They turn out to be simple polynomial functions of the streamwise (and corresponding integration) variables in the inviscid limit $\lambda\to 0$.

Classical Stuart–Watson–Landau theory suppresses the critical-layer effects, which can only be justified when the Reynolds number is assumed to be sufficiently small. For inviscidly unstable flows, this assumption is inconsistent with the locally parallel flow assumption[17–19] (which is required for the external flows that are of interest herein). In high-Reynolds-number viscously unstable flows, classical weakly nonlinear theory is (at best) restricted to a rather smallish region in the vicinity of the lower branch of the neutral stability curve, in which case the size of the upstream linear region would have to be excessively small. Moreover, nonlinearity usually occurs in the vicinity of the upper branch of the neutral stability curve in most of the relevant boundary-layer-type experiments.[20]

To be consistent with our requirement that the solution evolve from an initially linear stage, the amplitude Eqs. (13) and (14) usually have to be solved subject to the upstream boundary conditions,

$$\tilde{A}\to a^{(0)}e^{\tilde{\kappa}\tilde{x}},\quad \tilde{A}_0\to e^{\tilde{\kappa}_0\tilde{x}}\quad \text{as } \tilde{x}\to-\infty, \tag{15}$$

so that they match onto the linear, small growth-rate solution far upstream (but see Sec. VII for an important exception to this). Notice that only the first term on each of the right-hand sides of Eqs. (13) and (14) contributes to these equations when $\tilde{A}$ and $\tilde{A}_0$ are sufficiently small—as they are initially—and that (15) is then an exact solution to the resulting equations. We therefore refer to these terms as the linear growth-rate terms.

We include the linear phase shift $\tilde{\kappa}_{0i}$ to allow for an appropriate amount of wave-number detuning in the analyses, which means that the resonance (1) does not necessarily have to be exact and that the analysis actually applies to a relatively broad wave-number range about this resonance condition.

IV. THE MEAN FLOW CHANGE

A significant feature of the present analysis is that the nonlinear critical-layer interaction produces a spanwise-variable, mean-flow change

$$u=\epsilon\,\mathrm{Re}\,\bar{u}_0(y,x_0)e^{2iZ}, \tag{16}$$

that is of the same order as the oblique-mode instability wave [see Eq. (2)] that initially produces the interaction. However, the associated cross-flow velocities

$$v=\sigma\epsilon\left(\frac{\epsilon}{\sigma}\right)^{1/3}\mathrm{Re}\,\bar{v}_0e^{2iZ}$$

and

$$w=\epsilon\left(\frac{\epsilon}{\sigma}\right)^{1/3}\mathrm{Re}\,\bar{w}_0e^{2iZ} \tag{17}$$

turn out to be somewhat smaller than this.

The unexpectedly large value of the spanwise distortion of the streamwise flow might require some explanation. It occurs because the streamwise velocity fluctuation of the external linear flow has a singularity at the critical layer. This makes the lowest-order velocity fluctuation (asymptotically) much larger in the critical layer than in the external flow. This fluctuation is therefore able to generate higher-order nonlinear terms $\propto |A|^2$ that are of the same asymptotic order as the streamwise velocity fluctuation in the external flow.

The transverse velocity amplitude $\bar{v}_0$ is the product of a function of the slow variable x_0 and a function of the transverse coordinate y, which can be found by numerically solving an appropriate steady Rayleigh equation when $\sigma=1$ but is given by the analytical long-wave solution to that equation in the long-wavelength limit $\sigma\to 0$. In either case, the streamwise velocity amplitude $\bar{u}_0$ can then be calculated from

$$\frac{\partial \bar{u}_0}{\partial x_0}=-\frac{U'}{U}\bar{v}_0, \tag{18}$$

where, as indicated above, U is the locally parallel base flow of the shear layer, and the prime denotes differentiation with respect to y. The slowly varying amplitude factor is obtained by matching with the flow in the critical layer. The result is that

$$\bar{u}_0 \propto \int_{-\infty}^{\tilde{x}} dx_1(\tilde{x}-x_1) \times \int_{-\infty}^{x_1} dx_2\, e^{(-2\bar{\lambda}/3)(x_1-x_2)^3}|A(x_2)|^2, \tag{19}$$

where $\bar{\lambda}$ is a suitably renormalized variable corresponding to λ.

In the remainder of the paper, we discuss the implications of the fundamental Eqs. (13) and (14).

V. THE PURE OBLIQUE MODE INTERACTION

First, suppose that the scaled plane-wave amplitude A_0 (or equivalently $\tilde{A}_0$) is much less than that of the oblique mode during the nonlinear interaction process. This would be appropriate for the supersonic free-shear-layer and the zero-pressure-gradient, low-Mach-number, supersonic boundary-layer flows alluded to previously. The plane wave will then be small when nonlinear effects come into play, and the problem reduces to the one originally considered by Goldstein and Choi.[1] In this case, the resonance condition (1) need no longer be satisfied, and the second term can be neglected on the right-hand side of (13), which simply becomes

$$\frac{d\tilde{A}}{d\tilde{x}}=\tilde{\kappa}\tilde{A}+i\tilde{\gamma}\int_{-\infty}^{\tilde{x}}\int_{-\infty}^{x_1} K_2\tilde{A}(x_1)\tilde{A}(x_2)\tilde{A}^* \times(x_1+x_2-\tilde{x})dx_2\,dx_1. \tag{20}$$

The kernel function K_2 is quite complex when viscous effects are retained, as in Wu, Lee, and Cowley,[4] but in the inviscid limit originally considered by Goldstein and Choi,[1] it is simply

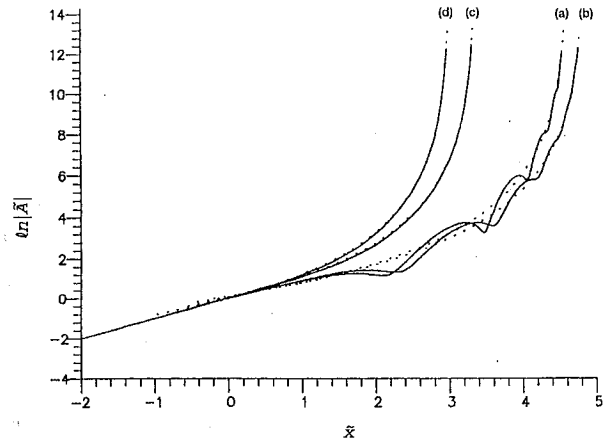

FIG. 5. Scaled amplitude $\ln|\tilde{A}|$ versus the scaled streamwise coordinate $\tilde{x}$ for $\tilde{\kappa}\tilde{\gamma}=1.2$: (a) $\theta=15°$; (b) $\theta=30°$; (c) $\theta=60°$; (d) $\theta=75°$. Solid lines: numerical solutions; dotted lines: local asymptotic solutions.

$$K_2=-\tfrac{1}{2}\tan^2\theta\cos 2\theta(\tilde{x}-x_1)[(\tilde{x}-x_1)^2+(\tilde{x}-x_2)^2 -\cos 2\theta(\tilde{x}-x_2)(x_1-x_2)]. \tag{21}$$

Plane-wave resonance effects only occur when $\theta=\pi/3$. In which case, the first two terms can be neglected on the right-hand side of (14). The plane wave will then be completely passive, will be driven by the oblique mode, and will evolve on the fast streamwise length scale $\tilde{x}_2=\tilde{x}/\delta_0$, where $\delta_0=O(\tilde{A}_0/\tilde{A})$.

The inviscid kernel function vanishes when $\theta\approx\pi/4$, and the inviscid solution to (20) develops a singularity at a finite downstream position,[1] say $\tilde{x}_s$, at all other angles. Therefore $\tilde{A}$ exhibits explosive growth at this point, and the local asymptotic expansion is given by

$$\tilde{A}\sim a/(\tilde{x}_s-\tilde{x})^{3+i\psi} \quad \text{as } \tilde{x}\to\tilde{x}_s, \tag{22}$$

where the real parameters a and ψ are related to the original parameters $\tilde{\kappa}$ and $\tilde{\gamma}$ through quadratures.[1]

Figure 5 is a plot of the scaled amplitude function $\tilde{A}$ versus the scaled streamwise coordinate $\tilde{x}$, as calculated numerically from Eqs. (20) and (21) for $\tilde{\kappa}\tilde{\gamma}=1.2$ and various values of θ. The curves show that the solution initially follows the linear growth given by

$$\frac{d\tilde{A}}{d\tilde{x}}=\tilde{\kappa}\tilde{A}, \tag{23}$$

and that the explosive growth occurs very suddenly once nonlinearity comes into play. The dashed curves are the local asymptotic expansions calculated from (22). This result implies that the overall wave-number/growth-rate scaling is preserved right up to the singularity when $\sigma=1$, which means that the overall asymptotic structure remains intact until the instability wave amplitude is $O(1)$ everywhere in the flow, and the motion will then be governed by the full nonlinear Euler equations in the next stage of evolution.

However, growth-rate amplitude scaling is not preserved in the long-wavelength limit $\sigma\to 0$ (corresponding to, say, a weak adverse-pressure-gradient boundary layer).

In this case, the critical layer expands to fill the wall layer, causing the flow to become fully nonlinear while the instability amplitudes are still small. The next stage of evolution is then characterized by a three-layer structure and is governed by the three-dimensional, unsteady "triple-deck" equations, but without the viscous terms. This does not, however, imply that the relevant scaling is the usual triple-deck scaling in this stage.

In any case, the next stage of evolution is always reached when the slow streamwise length scale is reduced to the order of the wavelength scale Δ/σ. It is therefore not very surprising that the full Euler equations are required when this latter length scale is of the order of the shear-layer thickness Δ and that the thin layer approximation to the Euler equations (i.e., the inviscid triple-deck equations) provides an adequate approximation when the wavelength is large compared to Δ.

Wu, Lee, and Cowley[4] showed that explosive growth also occurs in the viscous case and that the local asymptotic behavior in the vicinity of the singularity is still given by (22). However, they also showed that (as in Goldstein and Leib[21] and Leib[22]) there is a certain range of parameters where explosive growth does not occur when the viscous parameter λ exceeds a certain (usually very large) value. The instability wave will then reach a peak amplitude at some fixed streamwise location and subsequently undergo viscous decay downstream of that point.

Even more importantly, however, they show that the nonlinearly induced spanwise variable mean-flow change (16) does not decay in this case, but continues to grow linearly with x_0. It is easy to show that a new stage of evolution is then reached when $\epsilon x = O(1)$. The spanwise, variable, mean-flow change corresponding to (16) will then be $O[\sigma(\epsilon/\sigma)^{1/3}]$ in this stage. The resulting flow is affected by nonparallel effects and is governed by the linearized Navier–Stokes equations when $\sigma = 1$ and is unaffected by nonparallel mean-flow effects and is governed by the three-dimensional, linearized, triple-deck equations when $\sigma \to 0$.

Wu, Lee, and Cowley[4] also consider the strongly viscous limit of Eq. (20) by letting $\lambda \to \infty$ in this result. The corresponding initial (i.e., linear) critical layer is viscously dominated in this limit, which means that it is a balance between viscous diffusion and linear convection effects: It does not involve nonequilibrium or growth-rate effects. However, the ensuing nonlinear critical layer develops a double-layer structure, in this limit, with an inner viscous-dominated critical layer (in which the viscous forces again balance the convection effects) and (as in Goldstein and Hultgren[23]) an outer "diffusion layer" in which the spanwise variable mean-flow change is governed by the linear diffusion equation.

The most important result is that the nonlinear effects are completely determined by the flow in the diffusion layer to lowest-order approximation and are therefore affected by linear growth rate or nonequilibrium effects—just as they are in the $\lambda = O(1)$ case. This, in turn, implies that the corresponding evolution equation is still an integrodifferential equation in this limit. Namely,

$$\frac{d\hat{A}}{d\hat{x}} = \hat{\kappa}\hat{A} - i\tilde{\gamma}\tan^2\theta\sin^2\theta\cos 2\theta\left(\frac{1}{18}\right)^{1/3} \times \Gamma\left(\frac{1}{3}\right)\hat{A}\int_{-\infty}^{\hat{x}} |\hat{A}(x_1)|^2\, dx_1, \tag{24}$$

where Γ denotes the gamma function in the usual notation,

$$\hat{x} = \bar{\lambda}^{-1/3}\tilde{x}, \quad \hat{A} = \bar{\lambda}^{-1/3}\tilde{A}, \tag{25}$$

and we assume that

$$\hat{\kappa} \equiv \bar{\lambda}^{1/3}\tilde{\kappa} = O(1). \tag{26}$$

The viscous limit $\bar{\lambda} \to \infty$ is mainly of interest in flows where the wavelength σ^{-1} is also large—as will become clear when specific flows are discussed at the end of Sec. VII.

Equation (24) implies that

$$|\hat{A}| \propto e^{\hat{\kappa}\hat{x}} \quad \text{and} \quad \arg\hat{A} \propto e^{2\hat{\kappa}\hat{x}} \tag{27}$$

when $\hat{\kappa}$ and $\tilde{\gamma}$ are real—as they always are in the long-wavelength limit $\sigma \ll 1$. This means that the magnitude of $\hat{A}$ exhibits the same linear growth as in the nonresonant case, while its phase oscillates with increasing frequency as $\hat{x}$ becomes large. This reduction in streamwise length scale cannot, of course, persist indefinitely, and a new stage of development must eventually come into play. We anticipate that this latter stage will again be described by a limiting form of the general equation (13).

VI. THE PURE PARAMETRIC RESONANCE INTERACTION

Now consider the opposite limit where the scaled oblique-mode amplitude A is very small and remains that way during the entire resonant interaction. Notice that this includes the case

$$A = O(\epsilon/\sigma)^{1/3}, \tag{28}$$

where the oblique mode has the same amplitude scaling as the plane wave (as was originally pointed out by Goldstein and Lee[6]).

Equation (13) now becomes

$$\frac{d\tilde{A}}{d\tilde{x}} = \tilde{\kappa}\tilde{A} + i\int_{-\infty}^{\tilde{x}} K_1\tilde{A}_0(x_1)\tilde{A}^*(2x_1 - \tilde{x})\,dx_1, \tag{29}$$

while the plane-wave amplitude equation (14) reduces to the linear growth-rate equation

$$\frac{d\tilde{A}_0}{d\tilde{x}} = \tilde{\kappa}_0\tilde{A}_0, \tag{30}$$

which merely reflects the fact that there is no back-reaction of the oblique mode on the plane wave. It may seem rather surprising that this occurs even when the oblique-mode amplitude is of the same order as that of the plane wave, but the critical-layer velocity jump that would produce back-reaction at this level turns out to be identically zero.

Since the second member of the oblique-mode equation (29) is now linear in $\tilde{A}$, we refer to it as the parametric resonance term. Its kernel function is given by[24]

$$K_1 = \tfrac{3}{2}(\tilde{x} - x_1)^2 e^{-(2/3)\bar{\lambda}(\tilde{x}-x_1)^3}. \tag{31}$$

Goldstein and Lee[6] give an analytical solution to (29)–(31) for the inviscid limit $\bar{\lambda}=0$, and Wundrow, Hultgren, and Goldstein[25] extend it to the viscous case where $\bar{\lambda}=O(1)$. These solutions show that the oblique-mode instability-wave amplitude $\tilde{A}$ can be represented by a superposition of terms—each of which exhibits exponential growth. They also show that $\tilde{A}$ tends to be dominated by the lower-order terms at small values of $\tilde{x}$, but that the higher modes rapidly come into play and the "infinite tail" of the series eventually determines the behavior of the solution at large values of $\tilde{x}$. This leads to the conclusion that

$$\tilde{A}\sim c_0 e^{(i/2)\arg i\tilde{A}_0}e^{\tilde{\kappa}_{0r}\tilde{x}/5}e^{\int_{-\infty}^{\tilde{x}_0}(\tilde{A}_0/4)^{1/4}\,d\tilde{x}} \quad \text{as } \tilde{x}\to\infty, \tag{32}$$

provided that the shifting of the coordinate $\tilde{x}$ is correct to $O(\sigma)$ in the long-wavelength limit where $\sigma\ll 1$ and $\bar{\kappa}=\frac{4}{5}\bar{\kappa}_0$. Here, $\tilde{x}_0$ is a shifted coordinate corresponding to $\tilde{x}$, c_0 is a real constant, and $\tilde{A}_0$ is given by Eq. (30).

It is important to notice that $\tilde{A}_0$ [as given by Eq. (30)], will continue to grow (provided, of course, that $|\tilde{A}|$ remains sufficiently small) until the plane wave becomes strongly nonlinear within its own critical layer. This will occur when $\tilde{A}_0$ becomes $O(\sigma/\epsilon)^{2/3}$. Then, $\tilde{A}_0$ will evolve on the relatively slow scale $\tilde{x}$, but Eqs. (29) and (31) imply that $\tilde{A}$ must now evolve on the much faster scale $\tilde{x}(\sigma/\epsilon)^{1/6}$. The amplitude $\tilde{A}$ is then determined by appropriately rescaled versions of Eqs. (29) and (31), but with $\tilde{A}_0$ treated as a constant (or more correctly, a slowly varying function) and the linear growth-rate term missing. The critical-layer thickness that produces this result, and therefore governs the development of $\tilde{A}$, will now be much thicker than the plane-wave critical layer, which is of the same order as the original critical-layer thickness. The net result is that the amplitude $\tilde{A}$ is still determined by Eq. (32), but with the plane wave amplitude $\tilde{A}_0$ now given by the nonlinear critical-layer solution of Goldstein and Leib,[19] Goldstein and Hultgren,[23] Hultgren,[26] or Goldstein, Durbin, and Leib,[27] depending on the particular flow being considered. Since the oblique-mode amplitude is determined by Eq. (32) [and therefore satisfies Eq. (29)] in this stage of development, it will automatically match onto the full solution to Eqs. (29) and (31) when the appropriately shifted streamwise variable approaches upstream infinity, and the solution to these latter equations will then match onto the linear, small growth-rate solution farther upstream [i.e., it will satisfy the original upstream boundary condition (15)].

Notice that K_1 [as given by Eq. (31)] becomes highly concentrated around $\tilde{x}=x_1$ in the limit as $\bar{\lambda}\to\infty$. Equation (29) therefore reduces to the ordinary differential equation

$$\frac{d\hat{A}}{d\hat{x}}=\hat{\kappa}\hat{A}+\frac{3i}{4}\hat{A}_0\hat{A}^*, \tag{33}$$

where $\hat{x}$ and $\hat{A}$ are defined by Eq. (25) and

$$\hat{A}_0(\hat{x})\equiv\bar{\lambda}^{-2/3}\tilde{A}_0. \tag{34}$$

This is (to within a constant factor) the same as Craik's[5] equation, who used conventional Stuart–Watson–Laudau[14–16] theory to derive his result. Notice that the corresponding limiting form of the general plane-wave amplitude equation (13) is still the linear equation (30).

Equations (30), (33), and (34) imply that[5,25]

$$\hat{A}\sim\hat{C}_0 e^{i\pi/4}e^{\hat{\kappa}\hat{x}+(3/4\hat{\kappa}_{0r})e^{\hat{\kappa}_{0r}\hat{x}}} \quad \text{as } \hat{x}\to\infty, \tag{35}$$

where $\hat{C}_0$ is a real constant; we have chosen the origin of the $\hat{x}$ coordinates so that

$$\hat{A}_0=e^{\hat{\kappa}_{0r}\hat{x}} \tag{36}$$

and, for simplicity, we assume that $\hat{\kappa}_0$ is real.

Since Eq. (35) does not reduce to Eq. (32) in the limit $\bar{\lambda}\to\infty$, the limits $\bar{\lambda}\to\infty$ and $\tilde{x}\to\infty$ cannot be interchanged, and there must be some intermediate solution that connects Eqs. (32) and (35). In fact, it will be shown in a forthcoming paper by Wundrow, Hultgren, and Goldstein[25] that the approximation (33) becomes invalid when $\hat{\kappa}\hat{x}=0(\ln\bar{\lambda}^{2/3})$ and that the nonequilibrium effects become of the same order as the viscous effects for larger values of $\hat{x}$, at which point the flow begins to evolve on the faster scale

$$\bar{x}=\bar{\lambda}^{1/3}\left(\tilde{x}-\frac{1}{\tilde{\kappa}_{0r}}\ln\bar{\lambda}^{2/3}\right)=\bar{\lambda}^{2/3}\hat{x}_1, \tag{37}$$

where

$$\hat{x}_1\equiv\hat{x}-\frac{1}{\hat{\kappa}_{0r}}\ln\bar{\lambda}^{2/3} \tag{38}$$

is an appropriately shifted coordinate on the $\hat{x}$ scale, and is determined by the full nonequilibrium equation (29), but with $\hat{A}_0(\hat{x})$ treated as a slowly varying function of $\bar{x}$ and the linear growth term $\hat{\kappa}\hat{A}$ treated as a higher-order effect.

The relevant solution has the Wentzel–Kramers–Brillouin–Jeffreys (WKBJ) form and is easily shown to be

$$\bar{A}=C_0 e^{i\pi/4}\sqrt{\frac{b'}{b}}b^q e^{\bar{\lambda}^{2/3}\int_0^{\hat{x}_1}b(\xi)\,d\xi}, \tag{39}$$

where the prime denotes differentiation with respect to $\hat{x}$, b is determined by the transcendental equation

$$b(\hat{x}_1)=\frac{3}{2}\hat{A}_0(\hat{x}_1)\int_0^\infty e^{-(2/3)\zeta^3-2b(\hat{x}_1)\zeta}\zeta^2\,d\zeta, \tag{40}$$

$$\bar{A}\equiv\frac{1}{\bar{\lambda}}\tilde{A}, \tag{41}$$

and C_0 is a real constant. We have used the fact that $\tilde{A}_0$ satisfies Eq. (30) and have put $q\equiv\tilde{\kappa}/\tilde{\kappa}_0$.

Notice that

$$\hat{A}_0\to 0, \quad b\to 3\hat{A}_0/4$$

and, consequently, that

$$\bar{A}\to C_0(\tfrac{3}{4})^q\sqrt{\hat{\kappa}_{0r}}e^{i\pi/4}\exp\left[\hat{\kappa}\hat{x}_1+\frac{3}{4}\left(\frac{\bar{\lambda}^{2/3}}{\hat{\kappa}_{0r}}\right)(e^{\hat{\kappa}_{0r}\hat{x}_1}-1)\right]$$

$$\text{as } \hat{x}_1\to-\infty, \tag{42}$$

which shows that the solution (39) will match onto the asymptotic expansion (35) if we take

$$\hat{C}_0=\sqrt{\hat{\kappa}_{0r}}C_0(\tfrac{3}{4}\bar{\lambda}^{1/6})^q e^{-3\bar{\lambda}^{2/3}/4\hat{\kappa}_{0r}}. \tag{43}$$

VII. FULLY INTERACTIVE CASE

We now consider the fully coupled case where all the terms in (13) and (14) are of the same order. We have already discussed the significance of the various terms in (13), and the relevant kernel functions are given by (21) and (31). However, we have not, as yet, discussed the nonlinear terms in (14). They account for the back-reaction of the oblique mode on the plane wave—with the first group representing a kind of mutual interaction. The relevant kernel functions are given by[6]

$$K_3 = -6(\bar{x}-\tilde{x})^3 \tag{44}$$

and

$$K_4 = -3(\bar{x}-\tilde{x})(\bar{x}-x_1)(2\bar{x}-\tilde{x}-x_1) \tag{45}$$

in the inviscid limit.

The last term in Eq. (14), which is quartic in the oblique mode amplitudes, does not involve the plane-wave amplitude at all. It is worth noting that all previous analyses of the resonant-triad interaction (e.g., Craik,[5] and Smith and Stewart[28]) involve a corresponding back-reaction term that is, however, only quadratic in the oblique-mode amplitudes. The kernel function for this last term [of Eq. (14)] is given by[6]

$$K_5 = \tfrac{3}{4}(\bar{x}-\tilde{x})\{(\bar{x}+\tilde{x}+x_1-3x_2)(\bar{x}-x_2)(\bar{x}-2\tilde{x}+x_1) - (\bar{x}+\tilde{x}-2x_1)[(\bar{x}+\tilde{x}-2x_1)^2-3(\bar{x}-x_1)^2]\} \tag{46}$$

in the inviscid limit.

Most of the kernel functions have only been written down for the inviscid limit. However, they can, in principle, be modified to include viscosity, but some of the resulting formulas would then be exceedingly complex. It might therefore be best to account for viscous effects by numerically solving the relevant inhomogeneous critical-layer equations subject to the appropriate jump conditions. This is currently being done. Here we merely note that the resulting solutions will not be uniformly valid in frequency for the important class of weak, adverse-pressure-gradient, boundary-layer flows. This is because the viscous Stokes layer at the wall eventually contributes a term $(\sigma\bar{c})^3 U_c'^2/(\epsilon/\sigma)^{1/3}[2R(\omega^*\Delta/U_\infty)^5]^{1/2}$ to the scaled linear growth rate $\tilde{\kappa}_0$ when ω^* becomes sufficiently small. However, the solution can easily be made uniformly valid for all frequencies (except in the immediate vicinity of the lower branch) by simply replacing the linear growth rates in Eqs. (13) and (14) ($\tilde{\kappa}$ and $\tilde{\kappa}_0$, respectively) with

$$\tilde{\kappa} \to \tilde{\kappa} + \frac{4}{5}\frac{(\sigma\bar{c})^3 U_c'^2}{(\epsilon/\sigma)^{1/3}[R(\omega^*\Delta/U_\infty)^5]^{1/2}} \tag{47}$$

and

$$\tilde{\kappa}_0 \to \tilde{\kappa}_0 + \frac{(\sigma\bar{c})^3 U_c'^2}{(\epsilon/\sigma)^{1/3}[2R(\omega^*\Delta/U_\infty)^5]^{1/2}}. \tag{48}$$

Figure 6 (adapted from Ref. 6) shows a typical inviscid solution to Eqs. (13) and (14). It demonstrates that the oblique-mode amplitude initially exhibits linear growth, which is then accelerated in the so-called parametric resonance stage where the first "nonlinear" term comes into play in Eq. (13). Notice that the plane-wave amplitude continues to exhibit linear growth in this stage. However, the cubic self-interaction term quickly comes into play in (13), and a very rapid (explosive) growth of both the oblique mode and the plane wave then ensues: once the scaled oblique-mode amplitude becomes of the same order as that of the plane wave. (Notice that the unscaled oblique-mode amplitude is now much larger than that of the plane wave.) This is due to the presence of the singularity that arises from the oblique-mode self-interaction discussed in Sec. V. The back-reaction terms now transfer this singularity to the plane wave. The relevant local asymptotic expansion is still given by Eq. (22) for the oblique mode, while the corresponding result for the plane wave is given by[6]

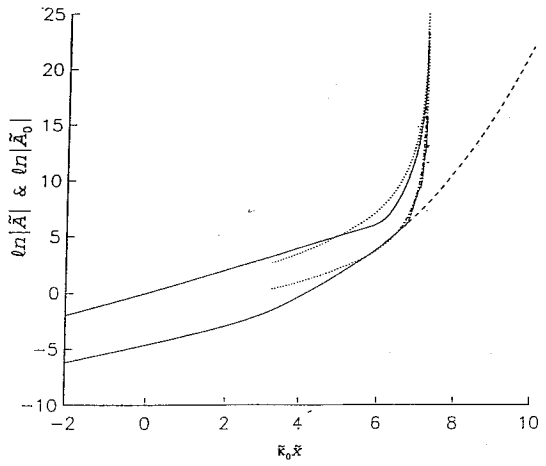

FIG. 6. $\ln|\tilde{A}|$ and $\ln|\tilde{A}_0|$ vs $\tilde{x}$. $|a^{(0)}|=0.01$, $\arg(a^{(0)})=0$, *and* $\tilde{\kappa}_i=0$ (solid: numerical; dotted: asymptotic; dashed: parametric-resonance; dot–dashed: linear 2-D case).

$$\tilde{A}_0 \sim \frac{a_0}{(\tilde{x}_s-\tilde{x})^{4+2i\psi}} \quad \text{as } \tilde{x}\to\tilde{x}_s. \tag{49}$$

These formulas were used to obtain the dotted curves in Fig. 6. Notice how quickly the solution reaches the asymptotic stage once the fully nonlinear cubic interaction terms come into play—especially for the oblique mode.

As in the pure oblique-mode interaction (discussed in Sec. V), the flow is again governed by the full Euler equations in the next stage of evolution when $\sigma=1$ and by the three-dimensional unsteady triple-deck equations (without the viscous terms) in the long-wavelength limit[6] $\sigma \ll 1$. (The underlying reasons are discussed in Sec. V.) Zhuk and Ryzhov[29] show that certain solutions to two-dimensional, unsteady inviscid triple-deck equations are determined by the Benjamin–Ono equation, which is known to possess solitary wave solutions. (A brief account of the three-dimensional case is given in a follow-up paper by Zhuk and Rzyhov.[30]) This suggests that the present solutions might also exhibit this behavior in the long-wavelength case and that this might play a role in the overall transition process in weak adverse-pressure-

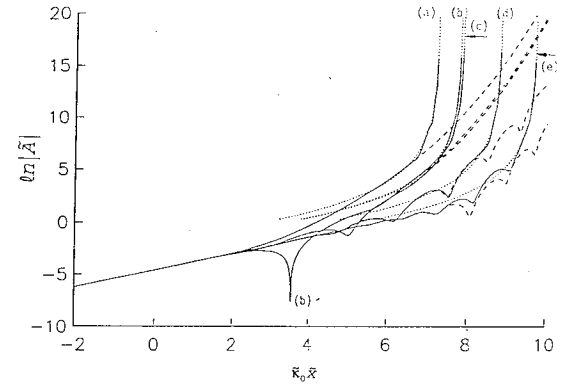

FIG. 7. $\ln|\tilde{A}|$ vs $\tilde{x}$. $|a^{(0)}|=0.01$, $\arg(a^{(0)})=0$, *and* $\tilde{\kappa}_i=0$, 1, 2, 4, 8, curves (a)–(e), respectively (solid: numerical; dotted: local asymptotic; dashed: parametric resonance).

gradient boundary layers.[31] The order-one wavelength solutions and subsequent full Euler behavior are probably more applicable to free shear layers than they are to boundary layers.

The dashed curve in Fig. 6 is calculated from the analytical solution for the parametric resonance stage that was discussed in Sec. VI. The dot–dashed curve is obtained by neglecting the back-reaction effects in (14), in other words, by using the appropriate linear solution of Eq. (30) to determine $\tilde{A}_0$ in Eq. (13). The close agreement with the exact solution is due to the fact that Eq. (30) provides the correct solution for $\tilde{A}_0$ in the parametric resonance stage, and the cubic nonlinear term, which does not involve $\tilde{A}_0$, becomes dominant as soon as the next stage of evolution is reached. This behavior, which seems to be quite typical for the inviscid case, may no longer obtain when viscous effects are included.

Figure 7 shows the effect of wave-number detuning on the oblique mode. It indicates that increased detuning (1) has the effect of delaying the onset of cubic nonlinearity and the attendant explosive growth, and (2) increases the oscillation in the amplitude curves. These oscillations are due to energy exchange between the various modes that interact nonlinearly within the critical layer. Figure 8 shows the corresponding result for the plane wave. Notice how abruptly the explosive growth sets in with large detuning.

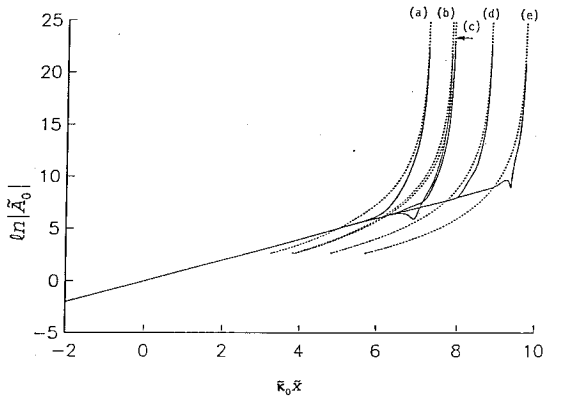

FIG. 8. $\ln|\tilde{A}|$ vs $\tilde{x}$. $|a^{(0)}|=0.01$, $\arg(a^{(0)})=0$, and $\tilde{\kappa}_i=0$, 1, 2, 4, 8, curves (a)–(e), respectively (solid: numerical; dotted: local asymptotic).

Equations (24) and (33) can be combined to show that

$$\frac{d\hat{A}}{d\hat{x}}=\hat{\kappa}\hat{A}+\frac{3i}{4}\hat{A}_0\hat{A}^*-i\hat{\gamma}\tan^2\theta\sin^2\theta \times\cos 2\theta\left(\frac{1}{18}\right)^{1/3}\Gamma\left(\frac{1}{3}\right)\hat{A}\int_{-\infty}^{\hat{x}}|\hat{A}(x_1)|^2dx_1, \tag{50}$$

in the viscous limit $\bar{\lambda}\to\infty$ with $\hat{\kappa}=O(1)$. Figure 9 is a plot, taken from Mankbadi, Wu, and Lee,[20] of some typical results computed from Eq. (50) with $\hat{\gamma}=1$ and $\theta=\pi/3$. It shows that the oscillations produced by the self-interaction term [see discussion following Eq. (27)] continuously reduce the parametric resonance effects to the point where the instability growth rate ultimately returns to its initial linear rate.

But Eq. (50) is not necessarily the only or even the most appropriate description of the fully interactive stage in the large $\bar{\lambda}$ limit. Notice, for example, that the parametric resonance solution (39) and (40) also applies to this limit. These equations show that the oblique mode continues to grow [when $\hat{A}_0$ is given by Eq. (30)] and therefore must eventually become large enough to react back on the plane wave and possibly interact nonlinearly with itself. The plane wave and oblique mode will then evolve on a much faster scale corresponding to $O(1)$ values of $\bar{x}$, as defined in Eq. (37).

The simplest way to show this is to notice that the viscous parameter $\bar{\lambda}$ can be scaled out of the general equations (13) and (14) by introducing the scaled dependent and independent variables (37), (41), and

$$\bar{A}_0\equiv\tilde{A}_0/\bar{\lambda}^{4/3} \tag{51}$$

and then replacing the linear growth rates $\tilde{\kappa}$ and $\tilde{\kappa}_0$ by the scaled growth rates $\tilde{\kappa}/\bar{\lambda}^{1/3}$ *and* $\tilde{\kappa}_0/\bar{\lambda}^{1/3}$, respectively. Then, aside from the vanishing of the linear growth-rate terms, the resulting equations will remain unchanged in the limit $\bar{\lambda}\to\infty$, with $\hat{\kappa}$ [as defined by Eq. (26)] and the barred variables held fixed. These latter equations do not possess solutions that satisfy the linear upstream boundary conditions (15), but they do possess solutions that satisfy the alternative conditions

$$\bar{A}\to\bar{a}^{(0)}e^{i\pi/4}e^{b_0\bar{x}},\ \bar{A}_0\to 1\quad\text{as}\ \bar{x}\to-\infty, \tag{52}$$

where

$$b_0\equiv\frac{3}{2}\int_0^\infty\zeta^2e^{-\zeta^3-2b_0\zeta}\,d\zeta, \tag{53}$$

and therefore match onto the limiting forms of parametric resonance solution (39) and (40) and the linear plane-wave solution

$$\bar{A}_0\equiv e^{\hat{\kappa}_0\hat{x}_1} \tag{54}$$

as the slow streamwise variable $\hat{x}_1\to 0$.

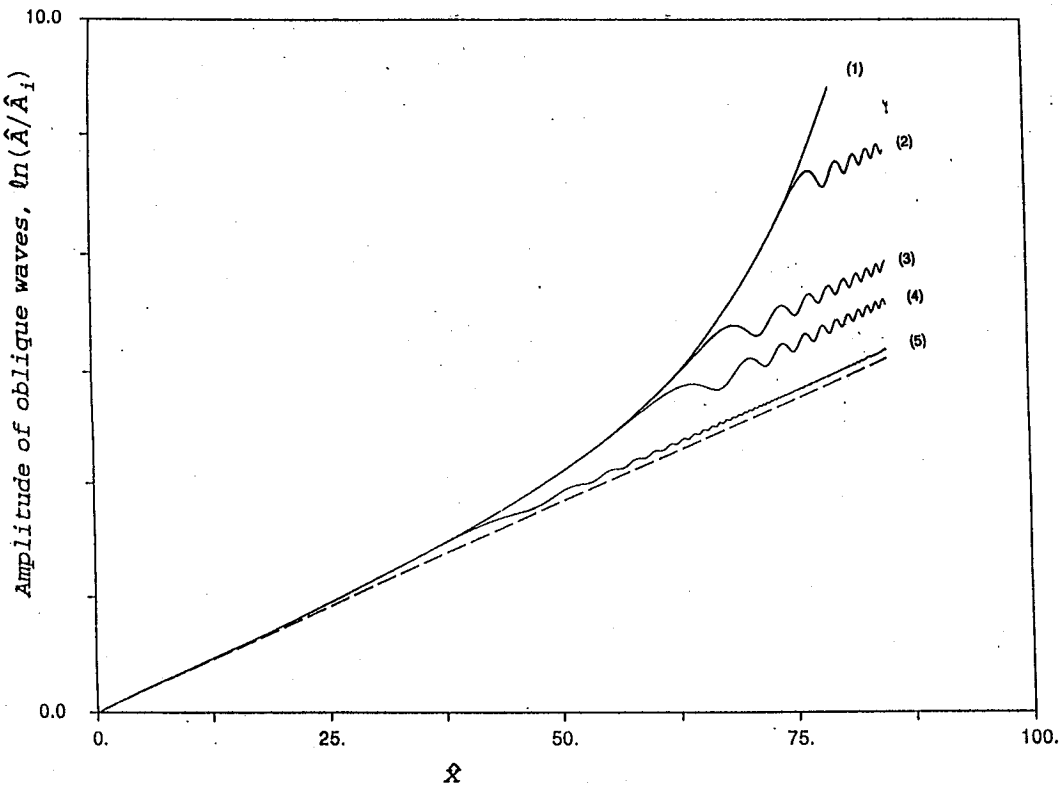

FIG. 9. Scaled amplitude $\ln \hat{A}/\hat{A}_i|$ versus scaled streamwise coordinate $\hat{x}$ for $\psi_{ei}=3\pi/2$. (1) Parametric resonance with self-interaction term set to zero. (2)–(5) Self-interaction accounted for: (2) $\hat{A}_i/\hat{A}_{oi}=0.1$, (3) $\hat{A}_i/\hat{A}_{oi}=0.5$, (4) $\hat{A}_i/\hat{A}_{oi}=0.9$, (5) $\hat{A}_i/\hat{A}_{oi}=5$; ----: linear solution.

The results of the previous section show that these latter solutions match onto an intermediate viscous parametric resonance stage and consequently onto the same upstream boundary conditions as Eq. (36) and the solution to Eq. (50) [i.e., Eq. (15) with the tilde replaced by a caret] provided, of course, that

$$a^{(0)}=O(\bar{\lambda}^{q/6}e^{-3\bar{\lambda}^{2/3}/4\hat{\kappa}_{0r}}). \tag{55}$$

This shows that the fully interactive stage is governed by the reduced viscous equations (30) and (50) whenever the oblique modes are only algebraically small relative to the plane wave at the start of parametric resonance, but the full nonequilibrium equations (13) and (14) are required whenever the oblique modes are exponentially smaller than the plane wave at the initiation of resonance. However, the smaller linear growth rate of the oblique modes could easily cause the latter situation to occur even when all the modes are of the same amplitude at the start of the linear stage. Evidently then, there is a kind of competition among modes in the initial linear stage that ultimately determines the nature of the flow in the fully interactive stage. Equation (50) will also be invalid when the plane wave becomes strongly nonlinear before back-reaction effects can occur—which means that competition between modes also occurs in the parametric resonance stage.

The main contribution to the inner integral in Eq. (19) comes from the vicinity of the point $x_2=x_1$ when $\bar{\lambda}\to\infty$, and it therefore follows from Eq. (25) that

$$\bar{u}_0\propto\bar{\lambda}\int_{-\infty}^{\hat{x}}(\hat{x}-\hat{x}_1)|\hat{A}(\hat{x}_1)|^2\,d\hat{x}_1=O(\bar{\lambda})\quad\text{as }\bar{\lambda}\to\infty. \tag{56}$$

Equations (50)–(56) apply to the Blasius boundary layer for which the amplitude wave-number scaling (11) obtains,[32] $R=O(\sigma^{-10})$, and $\omega^*\Delta/U_\infty=O(\sigma^2)$ over most of the unstable Reynolds number range. In which case, it follows from Eqs. (10) and (11) that $\epsilon=\bar{\lambda}\sigma^{10}$, and $\bar{\lambda}=\sigma^{-3/2}$, and, therefore [in view of Eq. (26)], that both terms on the right-hand side of Eq. (48) are of the same order. Equations (25), (34), (55), and (56) now imply that the oblique-mode, plane-wave, and spanwise variable mean-flow amplitude scalings are

$$\epsilon A=O(\epsilon\bar{\lambda}^{1/3})=O(\sigma^8)$$

or

$$\epsilon A\bar{\lambda}^{q/6}e^{-3\bar{\lambda}^{2/3}/4R_{0r}}=O(\sigma^{(8-q/4)}e^{-3/4\sigma R_{0r}}), \tag{57}$$

$$\epsilon(\epsilon/\sigma)^{1/3}A_0=O(\epsilon\bar{\lambda}\sigma^3)=O(\sigma^{10}), \tag{58}$$

and

$$\epsilon\bar{u}_0=O(\epsilon\bar{\lambda})=O(\sigma^7), \tag{59}$$

at the start of parametric resonance. The plane wave and oblique-mode amplitudes will be $O(\sigma^9)$ and $O(\sigma^7)$, respectively, in the fully interactive stage when the scaling (55)

applies. Equations (30) and (50) were first obtained by Mankbadi, Wu, and Lee,[20] who derived them directly from the Navier–Stokes equations.

Wu[9] shows that Eq. (50) also applies to accelerating boundary layers with $O(1)$ pressure gradients. In this case, $R=O(\sigma^{-6})$, $\omega^*\Delta/U_\infty$ is still[12] $O(\sigma^2)$, and the amplitude wave-number scaling (12) now applies over most of the unstable wave-number range. Then it follows from Eqs. (10) and (12) that $\epsilon=\sigma^{7/2}$, $\bar{\lambda}=\sigma^{-1/2}$, and, consequently, that both terms on the right-hand side of Eq. (48) are again of the same order. Equations (25), (34), (55), and (56) now show that the oblique-mode, plane-wave, and spanwise variable mean-flow amplitude scales are

$$\epsilon A=O(\epsilon\bar{\lambda}^{1/3})=O(\sigma^{10/3}) \tag{60}$$

or

$$\begin{aligned}&\epsilon\bar{\lambda}^{2/15}e^{-3\bar{\lambda}^{2/3}/4\hat{\kappa}_{0r}}=O(\sigma^{(1/3)(10-q/4)}e^{-3/4\sigma^{1/3}\hat{\kappa}_{0r}}),\\&\epsilon\left(\frac{\epsilon}{\sigma}\right)^{1/3}A_0=O\left(\frac{\epsilon(\sigma^{5/2})^{1/3}}{\sigma^{1/3}}\right)=O(\sigma^4),\end{aligned} \tag{61}$$

and

$$\epsilon\bar{u}_0=O(\epsilon\bar{\lambda})=O(\sigma^3), \tag{62}$$

at the start of parametric resonance.

However, in this case, Wu[9] shows that there is a thin diffusion layer near the wall where the mean flow distortion is even larger than this, namely $O(\sigma^{8/3})$. In any event, the important result is that the nonlinearly induced mean-flow distortion is always larger than the initial oblique-mode instability wave in the viscous limit $\bar{\lambda}\to\infty$, even in the main part of the shear layer. It is no coincidence that both of these flows correspond to the long wave limit $\sigma\to 0$, since viscous instabilities are always of the long-wavelength type at high Reynolds numbers.

VIII. CONCLUDING REMARKS

There are a large number of shear flows in which the oblique-mode instability waves exhibit the most rapid growth—either directly from the initial linear stage or indirectly through an intermediate parametric resonance stage. The cubic self-interaction between the oblique-mode instability waves is one of the first strictly nonlinear interactions to come into play as the instability waves evolve downstream in such flows. This interaction will have a dominant effect on the subsequent instability-wave development producing a local singularity (and consequently explosive growth) at a finite downstream position in the inviscid limit and sometimes producing viscous decay when viscosity is present.

The more or less general case is described by Eqs. (13) and (14), but depending on the initial amplitude ratio and the external parameters, various limiting forms of these equations can apply to different regions of the flow, giving rise to a wide variety of different phenomena. While these equations do not describe the nonlinear plane-wave behavior discussed in Sec. VI, arguments similar to those given in the previous section[6,25] show that even this strongly nonlinear flow eventually evolves into a fully interactive stage that is described by the weakly nonlinear equations (13) and (14) (but again with the linear growth terms omitted). The nonlinear interaction also produces a spanwise variable mean-flow change in the linear flow outside the critical layer, which is of the same order as the oblique-mode instability waves in the inviscid case and can be even larger than these in the strongly viscous case.

ACKNOWLEDGMENTS

The author would like to thank his colleagues, Dr. Sang Soo Lee, Dr. David Wundrow, Dr. Lennart Hultgren, Dr. Reda Mankbadi, and Dr. Stewart Leib, for their helpful comments during the course of this work.

[1] M. E. Goldstein and S. W. Choi, "Nonlinear evolution of interacting oblique waves on two-dimensional shear layers," J. Fluid Mech. **207**, 97 (1989); "Corrigendum," *ibid.* **216**, 659 (1989).
[2] C.-L. Chang and M. R. Malik, "Oblique mode breakdown in a supersonic boundary layer using nonlinear PSE," in *Instability, Transition, and Turbulence*, edited by M. Y. Hussaini, A. Kumar, and C. L. Street (Springer-Verlag, New York, 1992).
[3] A. Thumm, W. Wolz, and H. Fasel, "Numerical simulation of spatially growing three-dimensional disturbance waves in compressible boundary layers," in Proceedings of the Third IUTAM Symposium on Laminar–Turbulent Transition, Toulouse, France, 11–15 September 1989.
[4] X. Wu, S. S. Lee, and S. J. Cowley, "On the weakly nonlinear three-dimensional instability of shear layers to pairs of oblique waves: The Stokes layer as a paradigm," J. Fluid Mech. **253**, 681 (1993).
[5] A. D. D. Craik, "Nonlinear resonant instability in boundary layers," J. Fluid Mech. **50**, 393 (1971).
[6] M. E. Goldstein and S. S. Lee, "Fully coupled resonant-triad interaction in an adverse-pressure-gradient boundary layer," J. Fluid Mech. **245**, 523 (1992).
[7] T. Herbert, "Boundary-layer transition—analysis and prediction revisited," AIAA Paper No. 91-0737, 1991.
[8] P. R. Spalart and K. S. Yang, "Numerical study of ribbon-induced transition in Blasius flow," J. Fluid Mech. **178**, 345 (1987).
[9] X. Wu, "On critical-layer and diffusion-layer nonlinearity in the three-dimensional stage of boundary-layer transition," to appear in Proc. R. Soc. London Ser. A (1993).
[10] F. I. Hickernell, "Time dependent critical layers in shear flows on the beta-plane," J. Fluid Mech. **142**, 431 (1984).
[11] D. J. Benney and R. F. Bergeron, Jr., "A new class of nonlinear waves in parallel flows," Stud. Appl. Math. **48**, 181 (1969).
[12] W. H. Reid, "The stability of parallel flows," in *Basic Developments in Fluid Dynamics*, edited by M. Holt (Academic, New York, 1965), p. 249.
[13] D. J. Benney and S. A. Maslowe, "The evolution in space and time of nonlinear waves in parallel shear flows," Stud. Appl. Math. **54**, 181 (1975).
[14] J. T. Stuart, "On the nonlinear mechanics of wave disturbances in stable and unstable parallel flows. Part 1. The basic behaviour in plane Poiseuille flow," J. Fluid Mech. **9**, 353 (1960).
[15] J. Watson, "On the nonlinear mechanics of wave disturbances in stable and unstable parallel flows. Part 2. The development of a solution for plane Poiseuille flow and for plane Couette flow," J. Fluid Mech. **9**, 371 (1960).
[16] L. D. Landau and E. M. Lifshitz, *Fluid Mechanics*, 2nd ed. (Pergamon, London, 1987).
[17] P. Huerre, "The nonlinear stability of a free shear layer in the viscous critical layer regime," Philos. Trans. R. Soc. London Ser. A **293**, 643 (1980).
[18] P. Huerre, "On the Landau constant in mixing layers," Proc. R. Soc. London Ser. A **409**, 369 (1987).
[19] M. E. Goldstein and S. J. Leib, "Nonlinear roll-up of externally excited free shear layers," J. Fluid Mech. **191**, 481 (1988).
[20] R. R. Mankbadi, X. Wu, and S. S. Lee, "A critical-layer analysis of the resonant triad in boundary-layer transition," J. Fluid Mech. **256**, 85 (1993).

[21]M. E. Goldstein and S. J. Leib, "Nonlinear evolution of oblique waves on compressible shear layers," J. Fluid Mech. **207**, 73 (1989).
[22]S. J. Leib, "Nonlinear evolution of subsonic and supersonic disturbances on a compressible mixing layer," J. Fluid Mech. **224**, 551 (1991).
[23]M. E. Goldstein and L. S. Hultgren, "Nonlinear spatial evolution of an externally excited instability wave in a free shear layer," J. Fluid Mech. **197**, 295 (1988).
[24]M. E. Goldstein and S. S. Lee, "Oblique instability waves in nearly parallel shear flows," in *Nonlinear Waves and Weak Turbulence with Applications in Oceanography and Condensed Matter Physics*, edited by N. Fitzmaurice, D. Gurarie, F. McCaughan, and W. A. Woyczynski (Birkhäuser, Boston, 1993), p. 159.
[25]D. Wundrow, L. S. Hultgren, and M. E. Goldstein, "Interaction of oblique instability waves with a nonlinear plane wave," to appear in J. Fluid Mech. (1994).
[26]L. S. Hultgren, "Nonlinear spatial equilibration of an externally excited instability wave in a free shear layer," J. Fluid Mech. **236**, 497 (1992).
[27]M. E. Goldstein, P. A. Durbin, and S. J. Leib, "Roll-up of vorticity in adverse-pressure-gradient boundary layers," J. Fluid Mech. **183**, 325 (1987).
[28]F. T. Smith and P. A. Stewart, "The resonant-triad nonlinear interaction in boundary-layer transition," J. Fluid Mech. **179**, 227 (1987).
[29]V. I. Zhuk and O. S. Ryzhov, "Locally non-viscous perturbations in a boundary layer with self-induced pressure," Sov. Phys. Aerodyn. **27**, 177 (1982).
[30]V. I. Zhuk and O. S. Ryzhov, "Three-dimensional inviscid perturbances induced by the linear pressure gradient in a boundary layer," Sov. Phys. Dokl. **34**, 949 (1989).
[31]O. S. Ryzhov, "The formation of ordered vortex structures from unstable oscillations in the boundary layers," USSR Comput. Math. Phys. **30**, 146 (1990).
[32]M. E. Goldstein and P. A. Durbin, "Nonlinear critical layers eliminate the upper branch of spatially growing Tollmien–Schlichting waves," Phys. Fluids **29**, 2344 (1986).
[33]X. Wu, "The nonlinear evolution of high frequency resonant-triad waves in an oscillating Stokes layer at high Reynolds number," J. Fluid Mech. **245**, 553 (1992).